Original Article

Assessment of Four Scatter Correction Methods in In-111 SPECT Imaging: A Simulation Study

Mahsa Noori-Asl
Department of Physics, Faculty of Science, University of Mohaghegh Ardabili, Ardabil, Iran

Abstract

Introduction: Detection of compton scattered photons is one of the most important factors affecting the quality of single-photon emission computed tomography (SPECT) images. In most cases, the multiple-energy window acquisition methods are used for estimation of the scatter contribution into the main energy window(s) used in imaging. **Aims and Objectives:** The purpose of this study is to evaluate and compare the performance of four different scatter correction methods in In-111 SPECT imaging. Due to the lack of sufficient studies in this field, it can be useful to perform a more detailed and comparative study. **Materials and Methods:** Four approximations for scatter correction of In-111 SPECT images are evaluated by using the Monte Carlo simulation. These methods are firstly applied on each of photopeak windows, separately. Then, the effect of the correction methods is investigated by considering both the photopeak windows. The images obtained from a simulated multiple-spheres phantom are used for the evaluation of the correction methods by using three assessment criteria, including the image contrast, relative noise, and the recovery coefficient. **Results:** The results of this study show that the correction methods, when using the single photopeak windows, result in increase in image contrast with a significant level of noise. In return, when both the photopeak energy windows are used for imaging, it is possible to achieve the better image characteristics. **Conclusion:** The use of the proposed correction methods, by considering both the photopeak windows, leads to improve the image contrast with a reasonable level of image noise.

Keywords: Energy spectrum, indium-111, scatter correction, single-photon emission computed tomography

Received on: 30-01-2020 **Review completed on:** 12-04-2020 **Accepted on:** 29-04-2020 **Published on:** 20-07-2020

Introduction

The quality of images obtained from single-photon emission computed tomography (SPECT) imaging systems can be influenced by several factors; two most important of them are attenuation and scatter of photons emitted from the radionuclide used in the imaging. Whereas the attenuated photons do not arrive to the detector, and therefore, they have not any contribution in the final image, the scattered photons may arrive to the detector and be detect. Because these scattered photons have lower energy than the primary photons emitted from the radionuclide, they are often detected at energies lower than the photopeak energy. However, because of the limited energy resolution of the detection material used in gamma cameras (conventionally NaI (Tl) scintillation crystal), a number of scattered photons are always detected into the main energy window used in imaging, for example, in Tc-99m SPECT imaging, about 30%–40% of photons detected in the main energy window are scattered photons.[1] These scattered photons are added to the final image, resulting in image blurring and decreased image contrast. Therefore, for improvement of the diagnostic accuracy, it is necessary to find a suitable approach for reduction of the scattered photons included in the main energy window.

So far, many studies have been performed in the field of scatter correction in SPECT imaging. Most of these studies are related to the imaging with the radioisotope of technetium-99m.[2-18] There are a few studies for other radioisotopes. In this study,

Address for correspondence: Dr. Mahsa Noori-Asl, Department of Physics, Faculty of Science, University of Mohaghegh Ardabili, Ardabil, Iran.
E-mail: nooriasl.mahsa@gmail.com

Access this article online

Quick Response Code:

Website: www.jmp.org.in

DOI: 10.4103/jmp.JMP_5_20

How to cite this article: Noori-Asl M. Assessment of four scatter correction methods in in-111 SPECT imaging: A simulation study. J Med Phys 2020;45:107-15.

we intend to investigate and compare the influence of four scatter correction approximations on the quality of In-111 SPECT images. The indium-111 radioisotope decays by electron capture (EC) process to cadmium-111 with a half-life 67.9 h (2.8 days) that is suitable to use in SPECT imaging. During this decay, two gamma rays are emitted with energies 171 keV and 245 keV, both in high abundance [Figure 1].[19] Hence, dual-energy window settings are often used in In-111 SPECT imaging. In this study, first, the effect of interested scatter correction approximations on the each of photopeak energy windows is evaluated separately. Then, the scatter correction is performed by considering both photopeak windows.

In this study, we use the SIMulation of Imaging Nuclear Detectors (SIMIND) Monte Carlo simulation to generate the projection images. As, by using the simulation, it is possible to access the scattered and primary counts and also their spectra, independently, the simulation can be a suitable way for the investigation of the problem of scattering and the evaluation of performance of the scatter correction techniques. To evaluate the scatter correction methods, we used the simulated Jaszczak phantom including six spheres with different diameters placed into a cylindrical phantom. Two assessment criteria, image contrast and relative noise of background (RNB) together with the recovery coefficient (RC), are used for investigation of the effect of different scatter correction methods.

Materials and Methods

Scatter correction methods

Four methods for scatter correction of In-111 SPECT images are evaluated. First, this scatter correction methods are applied on each photopeak energy window, separately. In the next step, scatter correction is performed by considering both photopeak windows. The photopeak energy windows used in this study are including two 20% energy windows centered at energies 171 keV (154–188 keV) and 245 keV (221–269 keV), respectively.

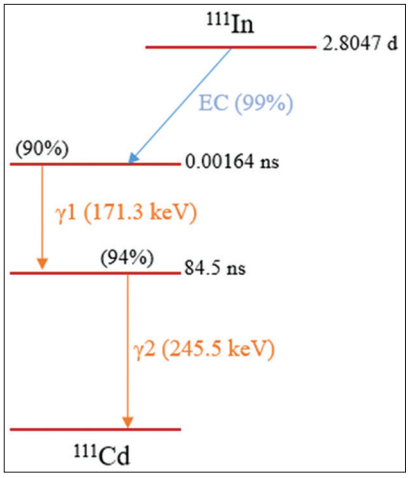

Figure 1: The decay scheme of In-111[19]

The scatter correction for each photopeaks window

Triple-energy window method for the first photopeak energy window (TEW-PK1)

In this approximation, the scatter counts detected into the first photopeak energy window (154–188 keV) are estimated by using a trapezoidal area. Total counts included into two narrow energy windows centered at energies 154 keV (T_{nw1}) and 188 keV (T_{nw2}) are used to estimate two heights of this trapezoid [Figure 2]. Therefore, the scatter counts of first photopeak window (S_{pk1}) can be estimated by the following equation (Eq. 1):[7]

$$S_{pk1}^{TEW}(i,j)=\left(\frac{T_{nw1}(i,j)}{w_{nw1}}+\frac{T_{nw2}(i,j)}{w_{nw2}}\right)\times\frac{W_{pk1}}{2} \quad (1)$$

Where w_{nw1} and w_{nw2} are the widths of narrow energy windows centered at energies 154 and 188 keV, respectively, and W_{pk1} is the width of the first photopeak window. (i,j) indicates the location of given pixel in the projection image matrix. In this approximation, two 8% and 6% narrow energy windows centered at the lower and upper energy limits of the first photopeak window are used.

Triple-energy window method for the second photopeak energy window (TEW-PK2)

In this approximation, it is assumed that there is no counts into the narrow energy window centered at the upper energy limit of the second photopeak window (i.e., energy 269 keV). Therefore, the scatter counts included into the second photopeak energy window (221–269 keV) can be estimated by using a triangular area that its height is determined by the total counts into a narrow window centered at energy 221 keV [Figure 3], as shown in the following equation (Eq. 2):

$$S_{pk2}^{TEW}(i,j)=\left(\frac{T_{nw3}(i,j)}{w_{nw3}}\right)\times\frac{W_{pk2}}{2} \quad (2)$$

Where w_{nw3} is the width of narrow energy window centered at energy 221 keV, and W_{pk2} is the width of the second photopeak energy window. In this approximation, a 6% narrow energy window centered at the lower energy limit of second photopeak window is used.

Dual-energy window method for the first photopeak energy window (DEW-PK1)

This scatter correction method is based on the dual-energy window method proposed by Jaszczak *et al*.[3,6] The essential assumption in this correction method is that the scatter counts into the photopeak window can be estimated as "*k*" times of the total counts acquired into a second energy window ($T1$) placed in the left side of the first photopeak window [Figure 4a]. Because almost all of the counts into this second energy window are the scatter counts, it is called as the "scatter window." Therefore, the scatter counts of the first photopeak window can be estimated as follows:

$$S_{pk1}^{DEW}(i,j)=k_{171}\times T_1(i,j) \quad (3)$$

According to the above equation (Eq. 3), the value of k factor can change pixel to pixel. Thus, a mean value of k is calculated and used in this scatter correction method. In this study, a scatter window with 20% width is used for the scatter correction.

Dual-energy window method for the second photopeak energy window (DEW-PK2)

Similar to the pervious method, the total counts into a 20% energy window ($T2$) placed in the left side of second photopeak window [Figure 4b] are used to estimate the scatter counts into this photopeak window:

$$S_{pk2}^{DEW}(i,j) = k_{245} \times T_2(i,j) \quad (4)$$

Scatter correction methods by considering both photopeak windows

Six-energy window method

This correction method is in fact a combination of triple-energy window (TEW) approximations used for two photopeak energy windows [Figure 5]. Therefore, the total number of scatter photons included into the both photopeak windows can be estimated by summing Eqs. (1) and (2), as follows:

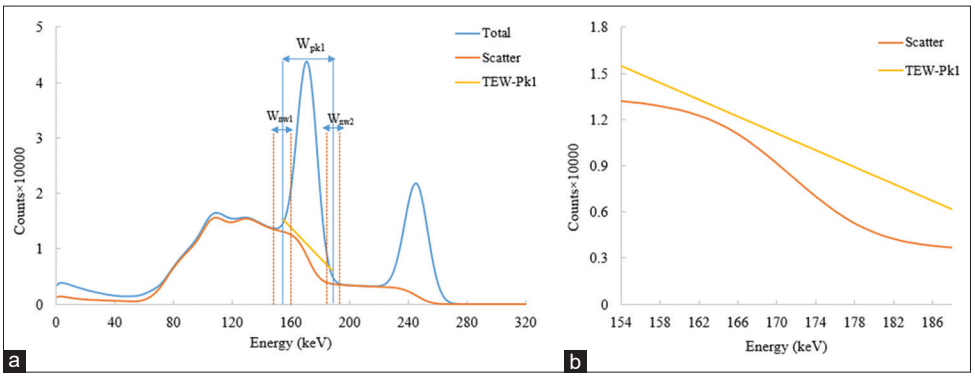

Figure 2: (a) The energy windows used in triple-energy window method by the trapezoidal approximation for the first photopeak window (154–188 keV). (b) The estimation of scatter area of the first photopeak window by the trapezoidal approximation along with the spectrum of true scatter counts into this energy window

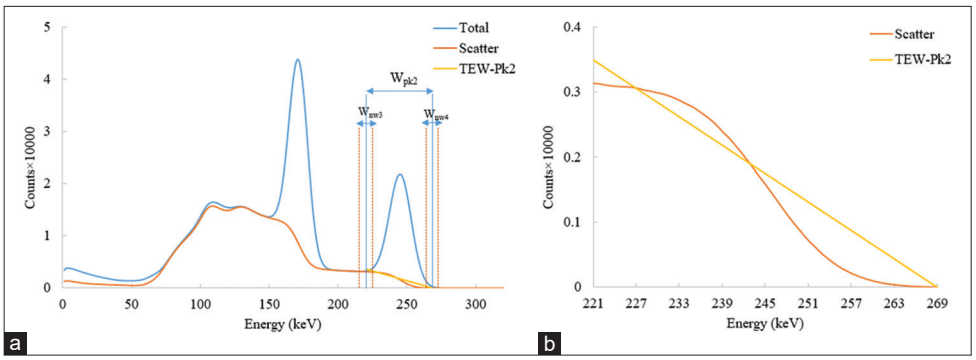

Figure 3: (a) The energy windows used in triple-energy window method by the trapezoidal approximation for the second photopeak window (221–269 keV). (b) The estimation of scatter area of the second photopeak window by the triangular approximation along with the spectrum of true scatter counts into this energy window

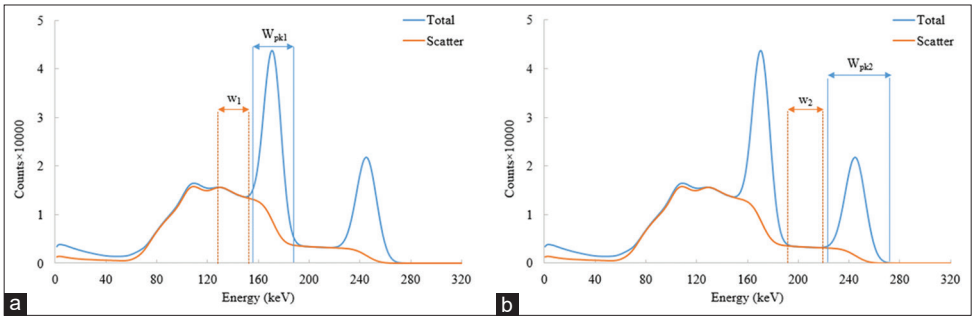

Figure 4: The energy windows used in dual-energy window method for (a) the first photopeak energy window and (b) the second photopeak window

$$S_{pk}^{SEW}(i,j) = S_{pk1}^{TEW}(i,j) + S_{pk2}^{TEW}(i,j) \quad (5)$$

Four-energy window method

This correction method is in fact a combination of dual-energy window approximations used for two photopeak energy windows [Figure 6]. Therefore, the total scattered counts can be estimated as follows:

$$S_{pk}^{FEW}(i,j) = S_{pk1}^{DEW}(i,j) + S_{pk2}^{DEW}(i,j) \quad (6)$$

Simulation

The SIMIND Monte Carlo program[20] (V.6.1.2 version), a MC code dedicated to simulate SPECT imaging, is used to produce the projection images from two photopeak energy windows and also, the narrow energy windows required to the scatter correction approximations. The simulated SPECT system is including a cylindrical NaI (Tl) crystal with radius 25 cm and thickness 0.95 cm, equipped to a general electric (GE) low-energy high-resolution parallel-hole collimator with the hexagonal holes. The system energy and intrinsic resolutions are 10% (FWHM) and 0.36 cm, respectively, for 140 keV. The projection images (128 × 128 matrices with a pixel size 0.3 cm) are acquired by a 360° rotation of camera with a radius of rotation 20 cm in 128 views. The image reconstruction is performed by using the filtered back-projection method with "Hann" filter in MATLAB (7.5.0 version) environment.

Simulated phantoms and assessment criteria

The phantom used in this study is a simulated model from the Deluxe Jaszczak phantom [Figure 7a] including six spheres with different diameters (3.2, 2.6, 2, 1.6, 1.3, and 1 cm) placed into a water-filled cylindrical phantom [Figure 7b]. This phantom can be simulated as both cold spheres in hot background phantom and hot spheres in cold background phantom, where "hot" and "cold" refer to the presence and absence of In-111 activity, respectively. This phantom is a basic phantom that has been used in many studies in the field of scatter and attenuation compensation.

Two mathematical criteria, including the image contrast and the RNB, are used to evaluate the images obtained from the cold spheres in hot background phantom. For calculation of these parameters, it is firstly necessary to define the regions of interest (ROIs) into each of the spheres and also into the background. These regions for largest to smallest spheres consist of 56, 30, 12, 10, 8, and 2 pixels, and for the background is a 16 × 16 matrix (256 pixels) defined in space between six spheres, as shown in Figure 7b. Accordingly, the assessment criteria are defined by the following equations (Eqs. 7 and 8):[14]

$$\text{Contrast} = \frac{\bar{N}_{CS} - \bar{N}_{BG}}{\bar{N}_{BG}} \quad (7)$$

$$\text{RNB} = \frac{\delta_{BG}}{\bar{N}_{BG}} \quad (8)$$

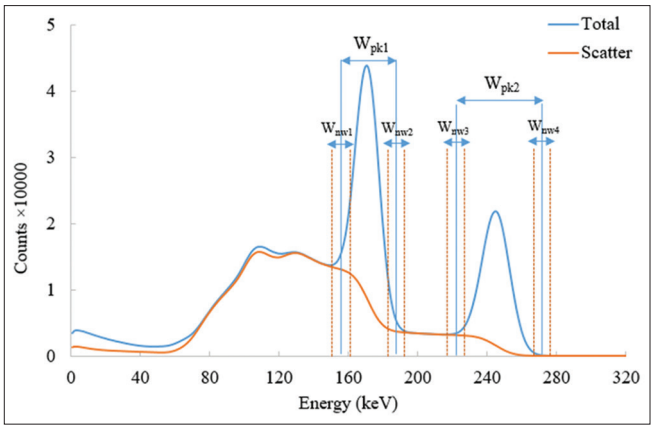

Figure 5: The energy windows used in six-energy window method defined as a combination of triple-energy window approximations used for two photopeak energy windows

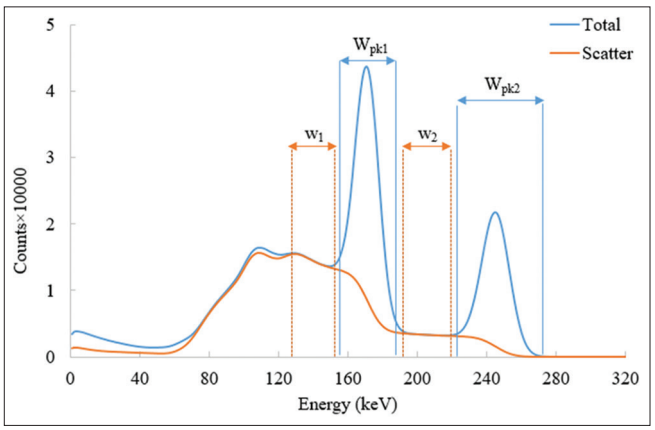

Figure 6: The energy windows used in four-energy window method defined as a combination of dual-energy window approximations used for two photopeak energy windows

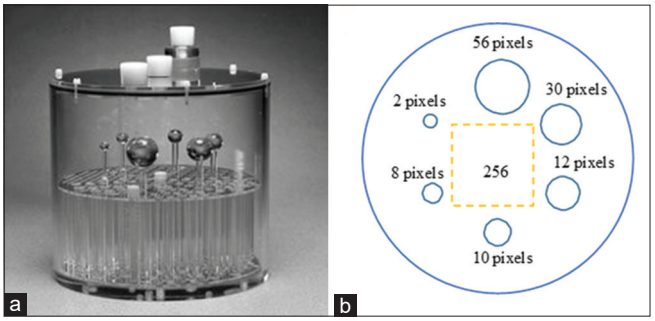

Figure 7: (a) The Deluxe Jaszczak phantom and (b) the cross section of simulated phantom including six spheres with different diameters (3.2, 2.6, 2, 1.6, 1.3, and 1 cm) placed into a water-filled cylindrical phantom together with the ROIs defined for the spheres and the background

Where $\bar{N}_{CS}$ and $\bar{N}_{BG}$ are the average of counts in ROIs defined for the spheres and the background, respectively, and δ_{BG} is standard deviation of the counts in ROI of the background.

On the other hand, the criterion used to evaluate the images results from the hot spheres in cold background phantom is recovery coefficient (RC) that is defined as follows:[15]

$$RC = \frac{\bar{N}_{HS}^{Corrected}}{\bar{N}_{HS}^{Primary}} \times 100 \quad (9)$$

Where $\bar{N}_{BG}^{Corrected}$ and $\bar{N}_{BG}^{Primary}$ are the average of counts in ROIs of the hot spheres corrected and primary images, respectively.

Results

The results of the simulation for cold spheres in hot background phantom show that about 32.5% of the photons acquired in the first photopeak energy window (154–188 keV) are the scattered photons, in which 72.6% undergo the first-order scattering, 22.0% the second-order scattering, and 5.4% the third-order scattering. On the other hand, for the second photopeak energy window (221–269 keV), 15.7% of the detected photons are the scattered photons, in which 91.8% undergo the first-order scattering, 7.7% the second-order scattering, and 0.4% the third-order scattering. These results indicate that most of the scattered photons in the second photopeak window are the first-order scattered photons. While for the first photopeak window, a significant number of scattered photons undergo the multiple scattering. The reason for this can be explained by using the relation of between energy and angle of Compton scattered photons as follows:[21]

$$E = \frac{E_0}{1 + (1 - \cos\theta)\frac{E_0}{m_e c^2}} \quad (10)$$

According to this equation (Eq 10), the 245 keV photons that undergo the first-order scattering with angle between 68.43° and 103.44° can be detected into the first photopeak window. It is clear that there is a chance for the multiple-scattered photons to fall into the first energy window in addition to the first-order scattered photons [Figure 8].

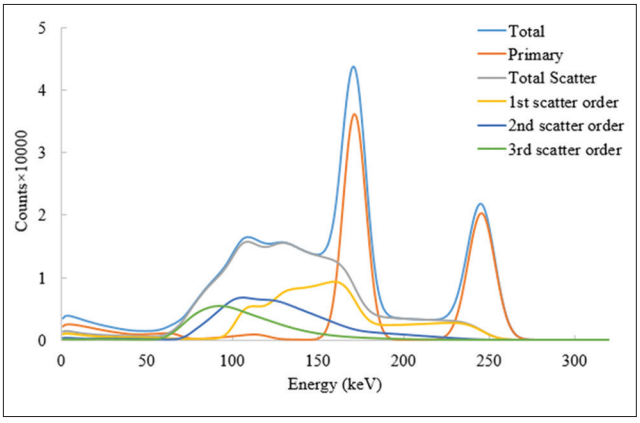

Figure 8: The spectra related to total (scatter + primary), primary (nonscattered), and total scatter (the sum of three scatter orders) counts along with the spectra of the first three scatter orders

The results for TEW correction method

The results obtained from the simulation of cold spheres in hot background phantom indicate that the true number of scattered photons included into the first and second photopeak energy windows are equal to 290,000 and 74,800, respectively. While the number of scattered photons estimated by the trapezoidal and triangular areas are about 371,308 and 84,685, respectively. From these results, the scatter correction by using the TEW method results in an overestimation of about 28% for the first photopeak window (Pk1) and 13.2% for the second photopeak window (Pk2). On the other hand, from Table 1, for both the photopeak windows, the use of the TEW correction method leads to improve the image contrasts of all of the cold spheres compared to before the correction (due to the low number of pixels included into the sphere with smallest diameter [sphere 6] and a lot of change in its contrast in different simulations, we discard from that). The relative increase of the image contrasts for largest to smallest spheres was about 41.46%, 38.20%, 22.50%, 11.71%, and 9.96% for the first photopeak window and 18.07%, 15.50%, 11.21%, 6.00%, and 3.15% for the second photopeak window. These results show that the relative increase of image contrasts for the first photopeak window is more than that of the second photopeak window. In addition, although the RNB obtained for the first photopeak window before correction (0.35) is about twice lower than the RNB for the second photopeak window (0.61), after scatter correction, the deference of these two values is low. This shows that the scatter correction by TEW method results in more increase of the level of noise in images obtained from the first photopeak window compared to the second photopeak window. A slice (slice 64) of the reconstructed images of cold-spheres for both the photopeak windows is shown in Figure 9. In addition, a similar slice of the reconstructed images of hot spheres along with a line profile through the center of spheres 1 and 4 are shown in Figures 10 and 11. From data given in Table 2, the RCs for the images of hot spheres corrected by TEW-Pk1 and TEW-Pk2 approximations are in the range of 10% lower and 2% higher than 100%, respectively, which indicate the corrected images of the second photopeak window have a

Table 1: The image contrast and the relative noise of background obtained from the reconstructed images of cold spheres in hot background phantom for two photopeak windows separately

Situation (RNB)	Spheres				
	S1	S2	S3	S4	S5
NC-Pk1 (0.035)	53.18	43.12	26.45	11.19	6.052
NC-Pk2 (0.061)	72.11	50.44	42.54	15.15	9.016
Primary-Pk1 (0.060)	83.39	68.64	47.05	20.53	9.128
Primary-Pk2 (0.070)	84.63	63.36	49.65	21.56	12.80
TEW-Pk1 (0.072)	91.84	77.99	48.37	22.28	16.01
TEW-Pk2 (0.078)	88.89	64.76	53.18	20.64	12.16
DEW-Pk1 (0.059)	87.12	71.49	45.96	18.52	12.42
DEW-Pk2 (0.076)	88.22	62.57	52.87	19.34	12.20

RNB: Relative noise of background, NC: No correction, TEW: Triple-energy window, DEW: Dual-energy window

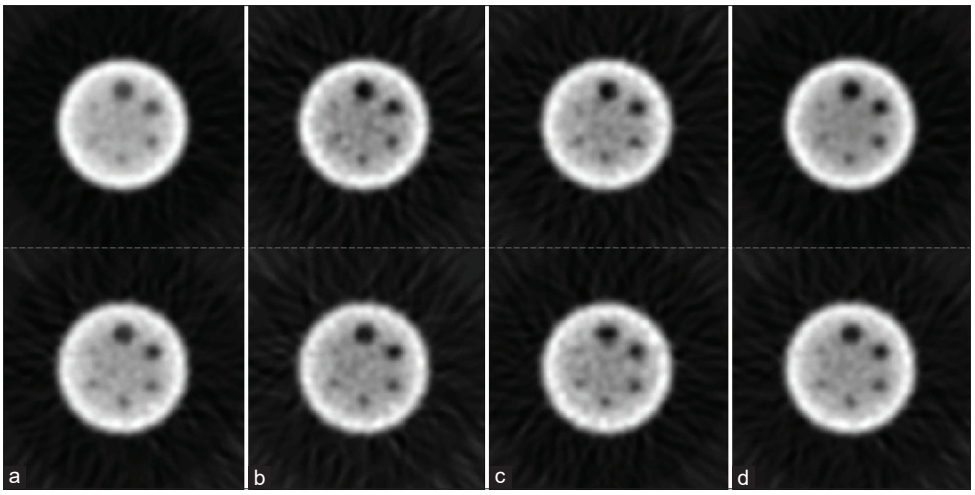

Figure 9: The reconstructed images of cold spheres in hot background phantom in four situations: (a) before correction, (b) corrected by triple-energy window method, and (c) corrected by dual-energy window method together with (d) the image obtained from the primary photons. The first and second rows are related to the first and second photopeak window, respectively

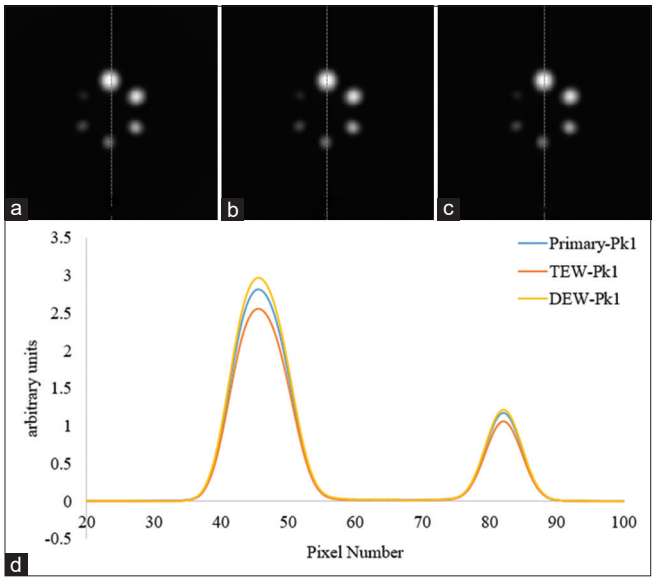

Figure 10: The reconstructed images of hot spheres in cold background phantom for the first photopeak windows in three situations: (a) the image result of the primary counts, (b) the image corrected by triple-energy window method, and (c) the image corrected by dual-energy window method together with (d) the line profiles obtained from a given row through the image of spheres 1 and 4

closer agreement with the primary images than that for the first photopeak window. These results are obvious from the profiles given in Figures 10d and 11d.

The results for DEW correction method

The first step in using the dual-energy window (DEW) correction method is to calculate the *k* factor for each of the photopeak windows. This factor is calculated by considering a 20% energy window in the vicinity of each of the photopeak windows so that the upper energy limit of these 20% windows is located on the lower energy limit of the photopeak windows. From the results of the simulation, the mean *k* values obtained for the first and second photopeak window are about 0.69 (with a minimum value 0.4232, maximum value 1.1585 and a standard deviation 0.0857) and 0.48 (with a minimum value 0.0596, maximum value of 1.2622, and a standard deviation of 0.1302), respectively. By using the calculated mean *k* values, the DEW correction method results in the relative increase of the cold sphere contrasts of about 36.45%, 30.48%, 20.61%, 7.29%, and 6.36% for the first photopeak window and about 17.47%, 13.07%, 10.74%, 4.21%, and 3.19% for the second photopeak window. Similar to TEW correction method, the use of this scatter correction method for the first photopeak window leads to a more relative increase of the cold sphere contrasts than that for second photopeak window. In addition, from the RNB values given in Table 1 for the first photopeak window, DEW correction method (DEW-Pk1) results in the lower level of image noise compared to TEW correction method (TEW-Pk2). On the other hand, from Table 2, the RCs of hot spheres by using both the DEW-Pk1 and DEW-Pk2 approximations are in a range of 6% higher than 100%, showing a similar agreement between the corrected and primary data for both photopeak windows [Figures 10d and 11d].

Results for SEW and FEW correction methods

Table 3 shows the results obtained from the six-energy window (SEW) and four-energy window (FEW) correction approximations. As expected, the RNB values obtained from these two correction approximations are significantly lower than the values result from approximations used for the single photopeak windows (the RNB value for the FEW correction approximation [0.049] is somewhat lower than that for the SEW correction approximation [0.0536]). Moreover, from the data of Table 3, the relative increase of the image contrasts for the largest to smallest cold spheres is about 33.35%, 29.04%, 19.19%, 9.56%, and 7.28% for the SEW correction approximation and

30.08%, 23.83%, 17.66%, 6.25%, and 5.26% for the FEW correction approximation, showing a more increase of image contrasts by using the SEW approximation than the FEW approximation. Figure 12 shows a slice of reconstructed images of cold spheres corrected by these two approximations. On the other hand, the RC values obtained from these two correction approximations show a range 6% lower and 6% higher than 100%, for SEW and FEW approximations, respectively. A slice of reconstructed images of hot spheres along with the line profiles through sphere 1 and 4 is shown in Figure 13.

Table 2: The recovery coefficients obtained from the reconstructed images of the hot spheres

Situation	Spheres				
	S1	S2	S3	S4	S5
TEW-Pk1	91.03	90.74	90.67	90.58	90.93
TEW-Pk2	101.78	101.48	101.16	101.26	101.14
DEW-Pk1	105.48	104.67	103.86	103.51	103.35
DEW-Pk2	105.46	104.53	103.56	103.08	103.10
SEW	95.37	95.06	94.86	94.84	94.97
FEW	105.46	104.53	103.56	103.08	103.10

TEW: Triple-energy window, DEW: Dual-energy window, SEW: Six-energy window, FEW: Four-energy window

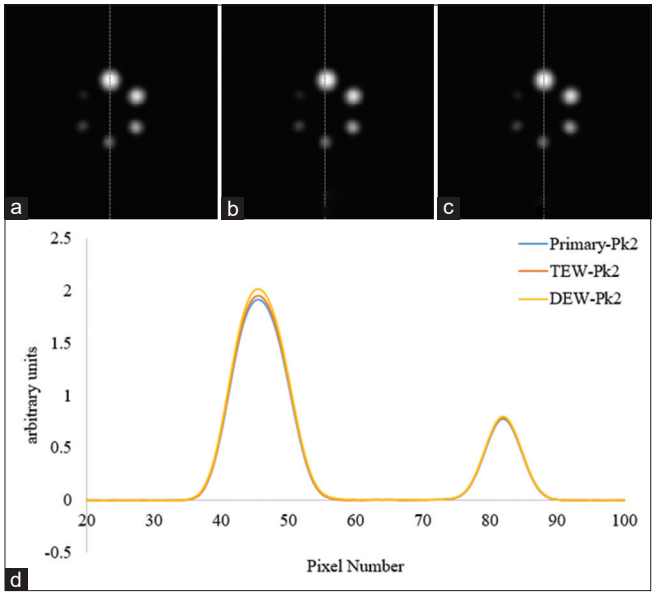

Figure 11: The reconstructed images of hot spheres in cold background phantom for the first photopeak windows in three situations: (a) the image result of the primary counts, (b) the image corrected by triple-energy window method, and (c) the image corrected by dual-energy window method together with (d) the line profiles obtained from a given row through the image of spheres 1 and 4

Discussion and Conclusion

Due to the importance of the problem of scattering and its effect on the quality of SPECT images, many studies have been conducted on the scatter correction techniques. Most of these studies are based on setting one or more additional energy windows in the spectrum of radioisotope used in imaging. Because Tc-99m is the most commonly used radioisotope in SPECT imaging, most of the proposed correction methods are based on the energy spectrum of this radioisotope. The correction approximations used for other radioisotopes are usually the modified methods used firstly in Tc-99m SPECT imaging.

In the present study, we investigated the effect of scatter correction on the SPECT images resulting from detection of the gamma rays emitted from the indium-111 radioisotope. It is important to note that the presence of two gamma photopeaks in the energy spectrum of indium-111 radioisotope results in the increase of the scatter contribution into the first photopeak window. This increase is due to fall down a number of scattered photons of the second photopeak window within the first photopeak window. This is why the scatter correction for the multiple-photopeak radioisotopes is more complicated than the single-photopeak radioisotopes.

There are a few studies in the field of the scatter correction in imaging with In-111 radioisotope. In an initial study performed by Gilland *et al.*,[22] the effect of the nonuniform attenuation correction using the transmission scan method (with a Tc-99m transmission source and a three-head camera) was compared to the uniform attenuation correction using the Chang method. In this study, in addition to two 20% photopeak windows, the other two energy windows positioned below each of the photopeak windows were used to estimate the scatter component into the corresponding photopeak windows. Based on the results of this study, the use of combined correction method (nonuniform attenuation correction + scatter correction) results in the

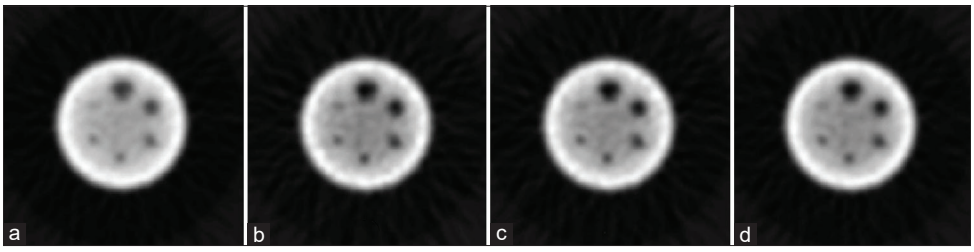

Figure 12: The reconstructed images of cold spheres in hot background phantom in four situations: (a) before correction, (b) corrected by six-energy window method, and (c) corrected by four-energy window method together with (d) the image obtained from the primary photons, by considering both the photopeak windows

Table 3: The image contrasts and the relative noise of background obtained from the reconstructed images of cold spheres in hot background phantom by considering both the photopeak windows

Situation (RNB)	Spheres				
	S1	S2	S3	S4	S5
NC (0.033)	59.56	45.59	31.88	12.53	7.052
Primary (0.050)	83.90	66.49	48.11	20.95	10.62
SEW (0.053)	90.55	72.21	50.48	21.56	14.33
FEW (0.049)	87.46	67.77	48.71	18.83	12.31

RNB: Relative noise of background, NC: No correction, SEW: Six-energy window, FEW: Four-energy window

improvement of the qualitative and quantitative accuracy of In-111 SPECT images. (These results are obtained in conditions where the combined projection data of two photopeak windows are used to produce the final image.) In another study, Penny *et al*.[23] used the dual-photopeak window (DPW) technique[9] for the scatter correction of the projection data of each of the photopeak windows. Moreover, they used a fifth energy window between two photopeak windows (W_5=195–225 keV) to estimate the scatter spill down from the second photopeak window into the first photopeak window. According to the results obtained from the point source imaging, this scatter correction approximation leads to reduction in the scatter fraction magnitude for both the photopeak windows. In another study, Choi *et al*.[24] investigated the effect of scatter correction on the projection data acquired from the second photopeak window by a 10% scatter window placed between two photopeaks at an energy of 205 keV using two ways: (1) the standard DEW correction method[3] and (2) a modified DEW method for accounting the contribution of the scattering into the detector crystal. The results of this study showed that except in cases that the scattering in the patient' body is very low, method 1 results in an accuracy equivalent to that for method 2. Finally, in the study performed by Holstensson *et al*.,[25] the optimal energy window settings for a camera with ability of the data acquisition in three energy windows were investigated. This study is only a comparative study performed in the field of scatter correction in In-111 SPECT imaging. In this study, first, the effect of scatter correction on each of the 20% photopeak windows was evaluated by using the TEW method.[7] In the next step, the effect of scatter correction on the combined data of the two photopeak windows was investigated by setting a third energy window in two different positions into the In-111 energy spectrum: (1) a 6% narrow energy window at 149 keV and (2) a 10% broad energy window at 209 keV. The results obtained from the experimental and simulation studies showed that the scatter correction of the combined data of two 20% photopeak windows using a 10% broad energy window at 209 keV can be an optimal energy window setting for In-111 SPECT imaging.

In the present study, an attempt has been made to investigate the scattering problem and also, the efficiency of scatter correction

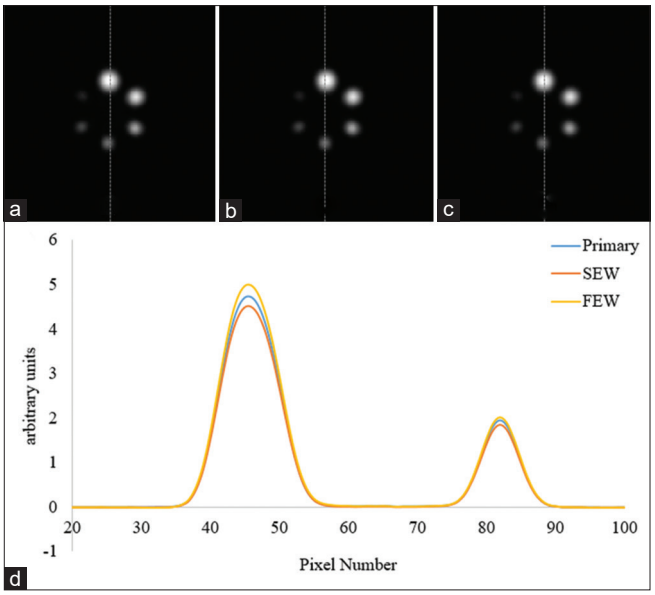

Figure 13: The reconstructed images of hot spheres in cold background phantom by considering both photopeak windows in three situations: (a) the image result of the primary counts, (b) the image corrected by six-energy window method, and (c) the image corrected by four-energy window method together with (d) the line profiles obtained from a given row through the image of spheres 1 and 4

techniques in In-111 SPECT imaging in more detail. For this purpose, in the first stage, we considered two photopeak windows independently and in the next stage, as combined together. The results obtained from the first stage indicate that the use of TEW and DEW correction methods results in the improvement of the cold sphere contrasts for the images from both photopeak windows, with a greater mean relative increase for the first photopeak window (24.76% for the TEW method and 20.24% for the DEW method) compared to the second photopeak window (10.78% for the TEW method and 9.37% for the DEW method). On the other hand, the relative increase of level of noise in the corrected images from the first photopeak window (51.4% for the TEW method and 40.7% for the DEW method) is significantly higher than that from the second photopeak window (21.8% for the TEW method and 19.7% for the DEW method), with a lower level for the DEW correction method compared to the TEW correction method. Furthermore, the RCs obtained from the hot sphere images show that contrary to the TEW method, the images corrected by the DEW method from two photopeak windows show a similar agreement with their primary images. Furthermore, the results obtained from the second stage indicate that the use of SEW and FEW correction approximations leads to an average of relative increase of about 19.68% and 16.61% for cold sphere contrasts and 37.7% and 32.6% for the level of image noise that is comparable to 34% for primary image.

As expected, the use of the collective photopeak window instead of the single photopeak windows led to decrease in the level of noise in In-111 SPECT images. Therefore, according to the results obtained from this study, we can introduce the

SEW and FEW approximations as two suitable methods for the scatter correction of In-111 SPECT imaging, with a greater mean relative increase of the cold sphere contrasts for the SEW approximation and a lower relative increase of level of noise for the FEW approximation. Therefore, the SEW correction approximation is preferred when the image contrast is an important parameter in imaging, and the FEW correction approximation is recommended when the low level of noise in SPECT images is desirable. In addition, because of the need of up to three energy windows for each photopeak energy, the proposed approximations are applicable in the clinical imaging systems.

Financial support and sponsorship

Nil.

Conflicts of interest

There are no conflicts of interest.

References

1. Hutton BF, Buvat I, Beekman FJ. Review and current status of SPECT scatter correction. Phys Med Biol 2011;56:R85-112.
2. Rydén T. Development of methods for analysis and reconstruction of nuclear medicine images. IEEE Trans Nucl Sci 1991;38:761-6.
3. Jaszczak RJ, Greer KL, Floyd CE Jr., Harris CC, Coleman RE. Improved SPECT quantification using compensation for scattered photons. J Nucl Med 1984;25:893-900.
4. Axelsson B, Msaki P, Israelsson A. Subtraction of Compton-scattered photons in single-photon emission computerized tomography. J Nucl Med 1984;25:490-4.
5. Floyd CE, Jaszczak RJ, Greer KL, Coleman RE. Deconvolution of Compton scatter in SPECT. J Nucl Med 1985;26:403-8.
6. Yanch JC, Flower MA, Webb S. A comparison of deconvolution and windowed subtraction techniques for scatter compensation in SPECT. IEEE Trans Med Imaging 1988;7:13-20.
7. Ogawa K, Harata Y, Ichihara T, Kubo A, Hashimoto S. A practical method for position-dependent Compton-scatter correction in single photon emission CT. IEEE Trans Med Imaging 1991;10:408-12.
8. Logan KW, McFarland WD. Single photon scatter compensation by photopeak energy distribution analysis. IEEE Trans Med Imaging 1992;11:161-4.
9. King MA, Hademenos GJ, Glick SJ. A dual-photopeak window method for scatter correction. J Nucl Med 1992;33:605-12.
10. Pretoris PH, van Rensburg AJ, van Aswegen A, Lötter MG, Serfontein DE, Herbst CP. The cannel ratio method of scatter correction for radionuclide image quantification. J Nucl Med 1993;34:330-5.
11. Buvat I, Rodriguez-Villafuerte M, Todd-Pokropek A, Benali H, Di Paola R. Comparative assessment of nine scatter correction methods based on spectral analysis using Monte Carlo simulations. J Nucl Med 1995;36:1476-88.
12. Changizi V, Takavar A, Babakhani A, Sohrabi M. Scatter correction for heart SPECT images using TEW Method. J Appli Clinical Med Phy 2008;9:136-40.
13. Islamian JP, Bahreyni Toossi MT, Momennezhad M, Zakavi SR, Sadeghi R. Monte Carlo study of the effect of backscatter materail thickness on 99mTc source response in single photon emission computed tomography. Iran J Med Phys 2013;10:69-77.
14. Noori-Asl M, Sadremomtaz A, Bitarafan-Rajabi A. Evaluation of six scatter correction methods based on spectral analysis in 99mTc SPECT imaging using SIMIND Monte Carlo simulation. J Med Phys 2013;38:189.
15. Noori-Asl M, Sadremomtaz A, Bitarafan-Rajabi A. Evaluation of three scatter correction methods based on estimation of photopeak scatter spectrum in SPECT imaging: A simulation study. Phys Med 2014;30:947-53.
16. Ghaly M, Links JM, Frey E. Optimization of energy window and evaluation of scatter compensation methods in myocardial perfusion SPECT using the ideal observer with and without model mismatch and an anthropomorphic model observer. J Med Imaging (Bellingham) 2015;2. pii: 015502.
17. Knoll P, Rahmim A, Gültekin S, Šámal M, Ljungberg M, Mirzaei S, *et al*. Improved scatter correction with factor analysis for planar and SPECT imaging. Rev Sci Instrum 2017;88:094303.
18. Rafati M, Rouhani H, Bitarafan-Rajabi A, Noori-Asl M, Farhood B, Ahangari HT. Assessment of the scatter correction procedures in single photon emission computed tomography imaging using simulation and clinical study. J Cancer Res Ther 2017;13:936-42.
19. Chiang C, Lin H, Lin C, Jan M, Chuang K. Simulation of Multi-Photon Emission Isotopes using Time-Resolved SimSET Multiple Photon History Generator. 4th International Conference on Advancements in Nuclear Instrumentation Measurement Methods and their Applications (ANIMMA), Lisbon; 2015. p. 1-5.
20. Ljungberg M, Strand SE. A Monte Carlo program simulating scintillation camera imaging. Comput Methods Programs Biomed 1989;29:257-72.
21. Knoll GF. Detection and Measurement of Radiation. New York: John Wiley and Sons; 1999.
22. Gilland DR, Jaszczak RJ, Turkington TG, Greer KL, Coleman RE. Quantitative SPECT Imaging with Indium-111. IEEE Trans Nucl Sci 1991;38:761-6.
23. Penney BC, Rajeevan N, Bushe HS, Hademenos G, King A. A Scatter Reduction Method for In-111 Scintigrams using Five Energy Windows. IEEE Nuclear Science Symposium and Medical Imaging Conference, 2-9 November, Santa Fe, New Mexico, USA; 1991.
24. Choi CW, Barker WC, Buvat I, Carrasquillo JA, Bacharach SL. Implications of dual-energy-window (DEW) scatter correction inaccuracies for 111In quantitative geometric mean imaging. Nucl Med Commun 1997;18:79-86.
25. Holstensson M, Hindorf C, Ljungberg M, Partridge M, Flux GD. Optimization of energy-window settings for scatter correction in quantitative ^{111}In imaging: Comparison of measurements and Monte Carlo simulations. Cancer Biother Radiopharm 2007;22:136-42.